Sympathetic Electromagnetically-Induced-Transparency Laser Cooling of Motional Modes in an Ion Chain

Y. Lin,[*] J. P. Gaebler, T. R. Tan, R. Bowler, J. D. Jost,[†] D. Leibfried, and D. J. Wineland

National Institute of Standards and Technology, 325 Broadway, Boulder, Colorado 80305, USA
(Received 26 November 2012; published 8 April 2013)

We use electromagnetically-induced-transparency laser cooling to cool motional modes of a linear ion chain. As a demonstration, we apply electromagnetically-induced-transparency cooling on $^{24}\text{Mg}^+$ ions to cool the axial modes of a $^9\text{Be}^+$-$^{24}\text{Mg}^+$ ion pair and a $^9\text{Be}^+$-$^{24}\text{Mg}^+$-$^{24}\text{Mg}^+$-$^9\text{Be}^+$ ion chain, thereby sympathetically cooling the $^9\text{Be}^+$ ions. Compared to previous implementations of conventional Raman sideband cooling, we achieve approximately an order-of-magnitude reduction in the duration required to cool the modes to near the ground state and significant reduction in required laser intensity.

One proposal for building a quantum information processor is to use trapped, laser-cooled ions [1–3], where internal states of the ions serve as individual qubits that are manipulated by laser beams and/or microwave radiation. The Coulomb coupling between ions establishes normal modes of motion; transitions involving both the qubit states and motional modes enable entangling gate operations between multiple qubits. For high-fidelity deterministic entangling gates, we require that the thermal or uncontrolled components of the relevant modes be in the Lamb-Dicke regime [2], where the amplitude of the ions' uncontrolled motion is much less than the effective wavelength of the coupling radiation [4]. For most experiments this means that the motion must be cooled to near the quantum-mechanical ground state, which has typically been achieved with sideband laser cooling [2,5,6]. Scaling can potentially be achieved by storing ions in multizone arrays where information is moved in the processor by physically transporting the ions [7,8] or teleporting [9].

Ion motion can be excited by ambient noisy electric fields and/or during ion transport [7]. Therefore, for lengthy algorithms, a method for recooling the ions is needed. This can be accomplished by combining the qubit ions with "refrigerant" ions that are cooled without disturbing the qubit states, but "sympathetically" cool the qubits through Coulomb coupling [7,8,10–15]. Demonstrations of this technique in information processing have so far used sideband cooling [10–14]. While effective, sideband cooling can typically cool only one mode at a time, due to the differences in mode frequencies and narrowness of the sideband transitions. Furthermore, in the case of stimulated-Raman transition sideband cooling [6], the laser-beam intensities and detuning must be sufficiently large to avoid heating from spontaneous emission. Importantly, in experiments performed in this scalable configuration, the time required for recooling has been the limiting factor [12,16] and leads to errors due to qubit dephasing [17]. A technique that can mitigate these problems is electromagnetically-induced-transparency (EIT)

laser cooling, described theoretically in Refs. [18,19] and demonstrated on a single ion in Refs. [20–22]. For EIT cooling, required laser intensities are relatively small and the cooling bandwidth is large enough that multiple modes can be cooled simultaneously. To demonstrate these features, we investigate EIT cooling of multiple modes of linear ion chains containing $^9\text{Be}^+$ and $^{24}\text{Mg}^+$ ions. EIT cooling is applied to the $^{24}\text{Mg}^+$ ions, which cools all modes along the axis of the chain to near the ground state, thereby sympathetically cooling the $^9\text{Be}^+$ ions. We realize significant reductions in cooling duration and required laser intensity compared to previous experiments that employed sideband cooling [11–14].

Following Ref. [19], consider the three-level Λ system comprised of the bare states $|g_1\rangle$, $|g_2\rangle$, and $|e\rangle$ shown in Fig. 1(a). For an ion at rest, laser beams with resonant Rabi rates Ω_1 and Ω_2 and equal detunings $\Delta_1 = \Delta_2 \equiv \Delta > 0$ dress the bare states such that the system relaxes to the "dark" steady state $|\psi_D\rangle = (\Omega_2|g_1\rangle - \Omega_1|g_2\rangle)/\Omega$ with $\Omega \equiv \sqrt{\Omega_1^2 + \Omega_2^2}$. Absorption from a weak (third) probe laser beam has a spectrum indicated in Fig. 1(b). The frequency shift between the absorption null and the relatively narrow peak on the right is

$$\delta = (\sqrt{\Delta^2 + \Omega^2} - \Delta)/2. \tag{1}$$

If the difference in k vectors for the two dressing beams has a component along the direction of a motional mode, ion motion will prevent it from being in the dark state. In the frame of reference of the ion, the laser beams appear to be frequency modulated at the mode frequency ω. For small amplitudes of motion such that the ion is in the Lamb-Dicke regime, the ion is probed by sidebands at frequencies $\Delta \pm \omega$. If conditions are such that $\delta \simeq \omega$, the upper sideband is resonant with the narrow feature on the right side of Fig. 1(b) and the ion can scatter a photon while simultaneously losing one quantum of motion, similar to more conventional sideband cooling. One advantage of the EIT scheme is that the width of the right-hand peak can be
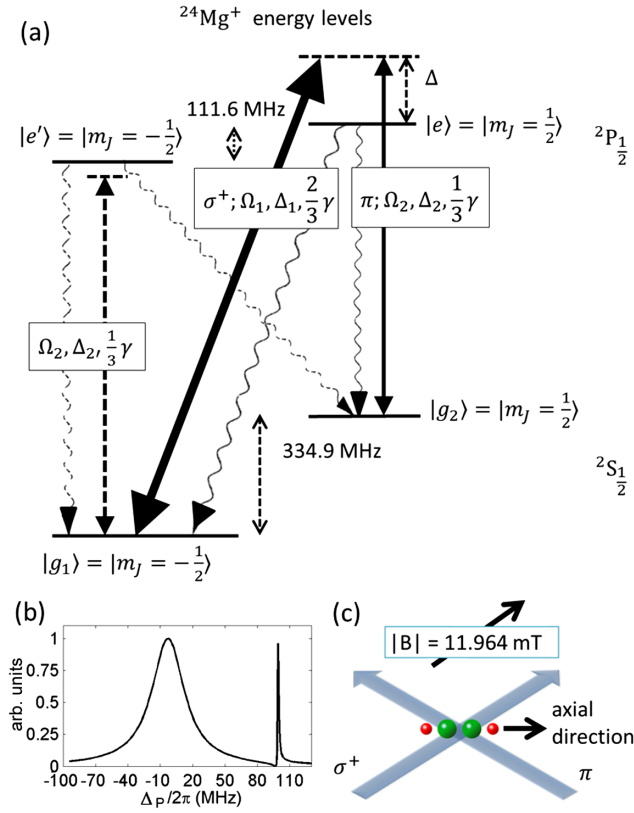
FIG. 1 (color online). (a) Relevant energy levels for $^{24}\text{Mg}^+$. The three levels $|g_1\rangle$, $|g_2\rangle$, and $|e\rangle$ serve as a Λ system for EIT cooling. Laser beams with σ^+ and π polarizations couple the ground states to the excited state with Rabi rates Ω_1 and Ω_2 and detuning Δ. Wavy lines show spontaneous emission from the excited state to the ground states and the excited-level decay rate is denoted with $\gamma \simeq 2\pi \times 41$ MHz. The fourth level $|e'\rangle$ can perturb the EIT cooling when the π polarized laser beam has frequency near the $|g_1\rangle$ to $|e'\rangle$ resonance. (b) Simulation of the absorption spectrum of a stationary ion by a weak probe beam for $\Delta = 2\pi \times 96.7$ MHz, $\Omega_1/2\pi = 30$ MHz, and $\Omega_2/2\pi = 12$ MHz. For simplicity, the fourth level $|e'\rangle$ is ignored for (b). The probe detuning from the $|g_2\rangle$ to $|e\rangle$ resonance is denoted by Δ_P. This Fano-like profile contains a narrow and broad feature corresponding to dressed states $|\psi_+\rangle$ and $|\psi_-\rangle$, respectively [19]. When $\Delta_P = \Delta$, absorption vanishes due to coherent population trapping. (c) Beam configuration and a depiction of the $^9\text{Be}^+$-$^{24}\text{Mg}^+$-$^{24}\text{Mg}^+$-$^9\text{Be}^+$ ion chain.

made broad enough that the condition for cooling is met for multiple modes for the same value of δ. This may prove advantageous in experiments involving many ions, such as simulations where the mode frequencies have a relatively narrow distribution [23–26].

We trap $^9\text{Be}^+$ and $^{24}\text{Mg}^+$ ions in a linear radio-frequency Paul trap described in Ref. [14]. The ions form a linear chain along the axis of the trap, the axis of weakest confinement, as depicted schematically in Fig. 1(c). We perform experiments on either a single $^9\text{Be}^+$-$^{24}\text{Mg}^+$ pair or a four-ion chain with the ions in the order $^9\text{Be}^+$-$^{24}\text{Mg}^+$-$^{24}\text{Mg}^+$-$^9\text{Be}^+$ [11,14]. A single trapped

$^9\text{Be}^+$ ion has motional frequency $\omega_z/2\pi = 2.97$ MHz along the trap axis and $\{\omega_x/2\pi, \omega_y/2\pi\} = \{12.4, 11.7\}$ MHz, along the transverse directions. An internal-state quantization magnetic field B is applied along a direction $45°$ to the trap axis [Fig. 1(c)], which breaks the degeneracy of magnetic sublevels of $^9\text{Be}^+$ and $^{24}\text{Mg}^+$. In Fig. 1(a), m_J indicates the projection of the $^{24}\text{Mg}^+$ ion's angular momentum along the direction of B. For $B = 11.964$ mT, the energy splitting of the qubit states $2s\,^2S_{1/2}|F = 2, m_F = 1\rangle$ and $|F = 1, m_F = 0\rangle$ of $^9\text{Be}^+$ is first-order insensitive to changes in B, leading to long coherence times of superposition states [17].

We apply two laser beams near the $3s\,^2S_{1/2}$ to $3p\,^2P_{1/2}$ transition in $^{24}\text{Mg}^+$ at approximately 280.353 nm [Fig. 1(a)]. These two beams are derived from the same laser and frequency shifted by acousto-optic modulators [27]. As indicated in Fig. 1(c), one of the beams propagates along the direction of B with σ^+ polarization to couple $|g_1\rangle$ to $|e\rangle$ with resonant Rabi rate Ω_1 and detuning Δ_1 from the excited state. The other beam has π polarization and couples $|g_2\rangle$ to $|e\rangle$ with resonant Rabi rate Ω_2 and detuning Δ_2. We set $\Delta_1 = \Delta_2 = \Delta$; ($\Delta/2\pi$ can be set to a precision of approximately 1.5 MHz.) The difference in wave vectors Δk_z of the two beams is parallel to the trap axis. The values of Ω_1 and Ω_2 are determined from measurements of the Rabi rate for Raman carrier transitions and the ac Stark shift from the σ^+ polarized beam when it is detuned from resonance.

We first apply Doppler cooling to $^9\text{Be}^+$, which initializes the temperatures of the axial modes of motion to near the Doppler limit ($\simeq \hbar\gamma_{\text{Be}}/(2k_B)$, where γ_{Be} is the $^9\text{Be}^+$ excited-state decay rate and k_B is Boltzmann's constant). We then apply the EIT cooling beams to $^{24}\text{Mg}^+$ for a cooling duration t_c. To determine the final mean motional-state quantum number $\bar{n}$ of the normal modes, we compare the strength of red and blue Raman sideband transitions in the $^9\text{Be}^+$ ions on the $|2, 1\rangle \rightarrow |1, 0\rangle$ transition, using a pair of 313.220 nm laser beams [6,28].

The $^9\text{Be}^+$-$^{24}\text{Mg}^+$ ion pair has two axial motional modes: a mode where the two ions oscillate in phase (I) with frequency $\omega_I/2\pi = 2.1$ MHz and an out-of-phase mode (O) with frequency $\omega_O/2\pi = 4.5$ MHz. The Lamb-Dicke parameters are defined as $\eta = \Delta k_z z_0$, where z_0 is the ground state mode amplitude for the $^{24}\text{Mg}^+$ ion; here, $\eta_I = 0.294$ and $\eta_O = 0.083$. The EIT cooling condition $\delta \simeq \omega$ cannot be satisfied for both modes simultaneously, since the mode frequencies are substantially different.

We first perform EIT cooling on $^{24}\text{Mg}^+$ for 800 μs, long enough for the system to reach equilibrium. We set $\Delta/2\pi = 96.7$ MHz and $\Omega_2/2\pi = 12.5$ MHz and scan the value of Ω_1 to vary δ [Eq. (1)].

The minimum values of $\bar{n}_I = 0.08(1)$ and $\bar{n}_O = 0.04(1)$ are obtained when δ closely matches the respective mode frequency, as expected [Fig. 2(a)]. We observe a $\simeq 10\%$
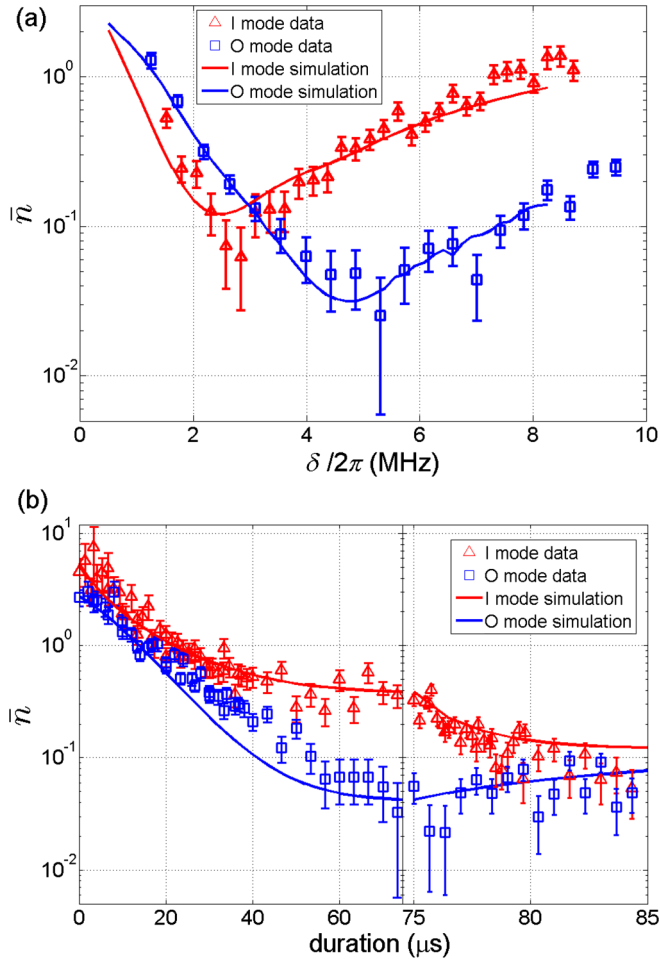
FIG. 2 (color online).   Mean motional excitation number $\bar{n}$ for the I (red triangles, $\omega/2\pi = 2.1$ MHz) and O (blue squares, $\omega/2\pi = 4.5$ MHz) axial modes of a $^9\text{Be}^+$-$^{24}\text{Mg}^+$ ion pair. (a) $\bar{n}$ after 800 μs of EIT cooling as a function of $\delta/2\pi$. Optimal cooling for each mode occurs when δ approximately equals the mode frequency. (b) $\bar{n}$ plotted as a function of EIT cooling duration t_c. From 0 to 74 μs, $\delta \simeq \omega_O$. From 75 to 85 μs, $\delta \simeq \omega_I$ (see text). In both figures, error bars represent statistical uncertainty of the sideband amplitude ratios. The solid lines are simulations of the full dynamics including the $|e'\rangle$ level in $^{24}\text{Mg}^+$, measured ambient heating rates, detuning and beam intensities. In the simulations, we truncated the motion to the first 6 Fock states for both modes for the steady-state simulation in (a) and to the first 10 (6) Fock states for I(O) mode for temporal simulation in (b).

deviation of the value of δ needed for optimum cooling compared to the mode frequency, which can be explained by additional ac Stark shifts and photon scattering from the π-polarized beam that couples $|g_1\rangle$ to $|e'\rangle \equiv {}^2P_{1/2}|m_J = -1/2\rangle$ in $^{24}\text{Mg}^+$ [see Fig. 1(a)]. We performed a numerical simulation of the full dynamics including state $|e'\rangle$. We also include the effects of heating rates of both modes, $\dot{\bar{n}}_I = 0.38$ quanta/ms and $\dot{\bar{n}}_O = 0.06$ quanta/ms. The average occupation numbers from the simulation are shown as solid lines in Fig. 2(a), and are in good agreement with

our experimental results. For the simulations, we use the treatment of Ref. [19], valid in the Lamb-Dicke regime, adjusted for the relevant modes and mode amplitudes of the $^{24}\text{Mg}^+$ ions.

To investigate the temporal dynamics of the cooling, we set δ to be near a mode frequency and measure $\bar{n}$ vs cooling duration t_c. We first Doppler-cool both modes with $^9\text{Be}^+$ reaching $\bar{n}_I \sim 5$ and $\bar{n}_O \sim 2$. We find that at the experimentally determined optimum values of $\delta/2\pi$ of 2.55(5) and 4.87(5) MHz, the $1/e$ cooling time for the I mode is 4(1) μs and for the O mode is 15(1) μs. The faster cooling rate for the in-phase mode is expected because of its larger $^{24}\text{Mg}^+$ Lamb-Dicke parameter. We can take advantage of the difference in equilibration times to efficiently cool both modes, as shown in Fig. 2(b). We first set $\delta \simeq \omega_O$ and apply cooling for 75 μs, yielding $\bar{n}_O = 0.04(1)$. During this stage, the I mode is cooled to $\bar{n}_I = 0.36(3)$. We then set $\delta \simeq \omega_I$ and apply the cooling beams for an additional 10 μs, reaching $\bar{n}_I = 0.08(1)$. In this second cooling stage, the O mode begins to heat to its equilibrium value of $\bar{n} = 0.19(3)$, shown in Fig. 2(a) for this value of δ. However in 10 μs, this heating is small, leading to a final value of $\bar{n}_O = 0.07(2)$. Therefore, this two-stage cooling enables cooling of both modes to near their minimum $\bar{n}$ values in 85 μs.

We also investigate sympathetic EIT cooling for the four-ion chain $^9\text{Be}^+$-$^{24}\text{Mg}^+$-$^{24}\text{Mg}^+$-$^9\text{Be}^+$. We label the four-ion axial modes $\{1, 2, 3, 4\}$, which have mode frequencies $\simeq \{2.0, 4.1, 5.5, 5.8\}$ MHz and corresponding $^{24}\text{Mg}^+$ Lamb-Dicke parameters $\{0.21, 0.12, 0.063, 0.089\}$. Figure 3 shows the final $\bar{n}$ of each mode vs $\delta/2\pi$ after 800 μs of cooling to ensure a steady state. We set $\Delta/2\pi = 96.7$ MHz, $\Omega_2/2\pi = 9.6$ MHz, and scan $\Omega_1/2\pi$ from 17 to 73 MHz. The EIT cooling bandwidth is sufficient such
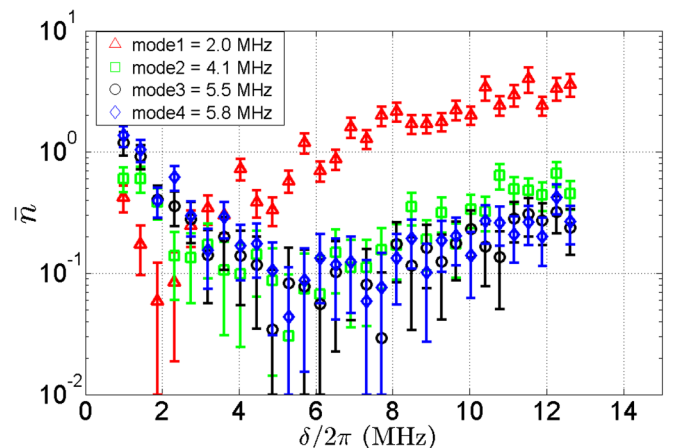

FIG. 3 (color online).   Minimum $\bar{n}$ values for each of the four axial modes of a $^9\text{Be}^+$-$^{24}\text{Mg}^+$-$^{24}\text{Mg}^+$-$^9\text{Be}^+$ ion chain as a function of $\delta/2\pi$ after 800 μs of cooling to ensure steady state. Modes 1 to 4 in the text are labeled as red triangles, green squares, black circles, and blue diamonds, respectively.
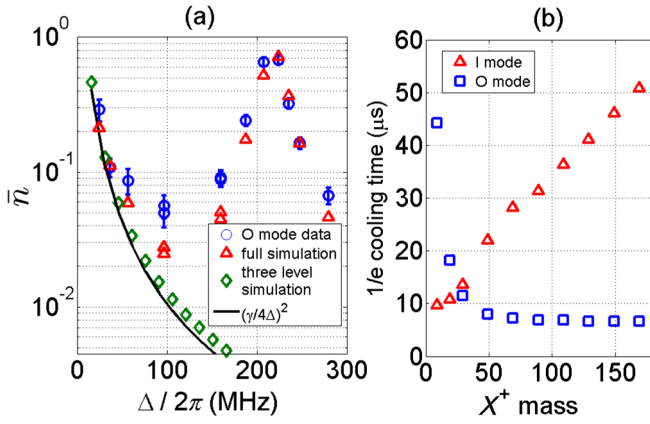
FIG. 4 (color online). (a) Minimum values of $\bar{n}$ for the two-ion O mode vs $\Delta/2\pi$. The peak near 223 MHz results from resonant scattering on the $|g_1\rangle \leftrightarrow |e'\rangle$ transition from the π polarized light. Blue circles are the experimental data and red triangles are simulations based on Ref. [19]. Green diamonds are simulations not including $|e'\rangle$ and the black solid line shows $\bar{n} = (\gamma/4\Delta)^2$ [18]. (b) Simulation of $1/e$ cooling time vs the mass of ion X^+ that is sympathetically cooled by $^{24}Mg^+$ (axial modes), with fixed trap potential such that $\omega_{I(O)}/2\pi = 2.1(4.5)$ MHz when X^+ is $^9Be^+$. Red triangles are for the I mode; blue squares for the O mode. Optimum values of δ were chosen for each mode and ion-mass combination, with $\Omega_2/2\pi = 5.9$ MHz and $\Delta/2\pi = 96.7$ MHz. (Here $|e'\rangle$ is neglected).

that modes 2, 3, and 4 can be simultaneously cooled to near their minimum $\bar{n} < 0.15$ by setting $\delta/2\pi = 6.1$ MHz; however, at this value, mode 1 is cooled only to $\bar{n} = 0.7(1)$. We therefore again cool in two stages: we apply 40 μs of cooling with $\delta/2\pi = 6.1$ MHz to cool modes 2, 3, and 4 followed by 5 μs of cooling with $\delta/2\pi = 2.4$ MHz to cool mode 1, reaching $\bar{n} = \{0.11(2), 0.20(5), 0.14(5), 0.18(5)\}$. In our experiments, laser beam power of the pi(sigma)-polarized beam ranged between 3 and 10 μW (3 and 17 μW). In previous implementations of sequential Raman sideband cooling [11–13,16], cooling of these modes from Doppler temperatures to $\bar{n} \sim 0.1$ for each mode required ~ 600 μs with approximately an order of magnitude higher laser intensities.

The $|g_1\rangle$ to $|e'\rangle$ transition frequency is 223.3 MHz higher than that of the $|g_2\rangle$ to $|e\rangle$ transition. Thus, EIT cooling will be strongly affected for $\Delta/2\pi$ near 223.3 MHz due to recoil from scattering on the $|g_1\rangle$ to $|e'\rangle$ transition. To illustrate the effect, we measure the minimum value of $\bar{n}$ for cooling the O mode of the $^9Be^+$-$^{24}Mg^+$ ion pair as a function of the detuning Δ [Fig. 4(a)]. For each value of Δ we optimize the EIT cooling by varying δ. The height of this recoil peak depends on the Rabi rate ratio Ω_2/Ω_1 with higher ratios leading to higher values of $\bar{n}$. For data of Fig. 4(a), the ratio was held at 0.24. We note that for large detuning Δ, higher laser intensity is needed to maintain values of δ near the mode frequencies.

When Δk_z is aligned along the trap axis, the motional modes along the transverse axes are heated by photon recoil. To study this effect, we first cool one of the transverse modes of a $^9Be^+$-$^{24}Mg^+$ pair (frequency $\simeq 4.6$ MHz) to near its ground state with Raman sideband cooling on $^9Be^+$. We then apply an EIT cooling pulse on the O mode, with similar laser beam conditions as above. After 60 μs, the O mode is cooled from the Doppler temperature ($\bar{n} \simeq 2$) to $\bar{n} = 0.04(1)$, while the transverse mode is heated from $\bar{n} = 0.20(6)$ to $0.9(2)$. Once the O mode is cooled to near its minimum value, the heating rate of the transverse mode decreases because the ion becomes approximately trapped in the dark state for spin and the ground state of axial motion. This relatively low transverse excitation should cause a negligible error on a two-qubit gate, which is affected by the transverse modes only through second-order coupling to the axial mode frequencies [29]. Furthermore, Doppler cooling of all modes before EIT cooling would prohibit any cumulative effect of the heating in experiments requiring many rounds of sympathetic cooling.

To study the efficiency of EIT sympathetic cooling on other ion species, such as $^{27}Al^+$, $^{43}Ca^+$, $^{171}Yb^+$, etc., we simulate cooling of an ion pair $^{24}Mg^+$-X^+, where X^+ is the sympathetically cooled ion of different mass, as shown in Fig. 4(b). Smaller differences in ion mass lead to more balanced mode amplitudes and a reduction in the difference of cooling rates for individual modes. Large mass imbalances lead to at least one motional mode having a small $^{24}Mg^+$ amplitude and, thus, a long cooling time [15].

In summary, we have described sympathetic cooling of $^9Be^+$ ions by EIT cooling of $^{24}Mg^+$ ions held in the same trap. We investigate the cooling for both an ion pair and a four-ion chain crystal that can be used as a configuration for performing entangling gates between pairs of $^9Be^+$ ions in a scalable architecture [11–13]. By taking advantage of the different cooling rates for different modes of motion, we demonstrated a two-stage EIT cooling scheme that can bring all modes to near their minimum excitation level. Compared to previous implementations of conventional Raman sideband cooling, sympathetic EIT cooling provides a broad cooling bandwidth, requires less laser power, and is technically easier to implement. This method may also be useful for sympathetic cooling of molecular ions, for use in quantum logic spectroscopy [10], trapped-ion quantum simulation [23–26], strongly confined neutral atoms [30], and nanomechanical resonators [31].

*yiheng.lin@nist.gov

†Present address: École Polytechnique Fédérale de Lausanne, CH-1015 Lausanne, Switzerland.

[1] J. I. Cirac and P. Zoller, Phys. Rev. Lett. **74**, 4091 (1995).

[2] R. Blatt and D. Wineland, Nature (London) **453**, 1008 (2008).

[3] R. Blatt and C. F. Roos, Nat. Phys. **8**, 277 (2012).

[4] Probabilistic schemes for entanglement do not require such strong confinement; see C. Monroe, R. Raussendorf, A. Ruthven, K. R. Brown, P. Maunz, L.-M. Duan, and J. Kim, arXiv:1208.0391.

[5] F. Diedrich, J. C. Bergquist, W. M. Itano, and D. J. Wineland, Phys. Rev. Lett. **62**, 403 (1989).

[6] C. Monroe, D. M. Meekhof, B. E. King, W. M. Itano, and D. J. Wineland, Phys. Rev. Lett. **75**, 4714 (1995).

[7] D. J. Wineland, C. Monroe, W. M. Itano, D. Leibfried, B. E. King, and D. M. Meekhof, J. Res. Natl. Inst. Stand. Technol. **103**, 259 (1998).

[8] D. Kielpinski, C. Monroe, and D. J. Wineland, Nature (London) **417**, 709 (2002).

[9] D. Gottesman and I. L. Chuang, Nature (London) **402**, 390 (1999).

[10] P. O. Schmidt, T. Rosenband, C. Langer, W. M. Itano, J. C. Bergquist, and D. J. Wineland, Science **309**, 749 (2005).

[11] J. D. Jost, J. P. Home, J. M. Amini, D. Hanneke, R. Ozeri, C. Langer, J. J. Bollinger, D. Leibfried, and D. J. Wineland, Nature (London) **459**, 683 (2009).

[12] J. P. Home, D. Hanneke, J. D. Jost, J. M. Amini, D. Leibfried, and D. J. Wineland, Science **325**, 1227 (2009).

[13] D. Hanneke, J. P. Home, J. D. Jost, J. M. Amini, D. Leibfried, and D. J. Wineland, Nat. Phys. **6**, 13 (2009).

[14] J. D. Jost, Ph.D. thesis, University of Colorado, Boulder, 2010.

[15] J. B. Wübbena, S. Amairi, O. Mandel, and P. O. Schmidt, Phys. Rev. A **85**, 043412 (2012).

[16] J. P. Gaebler, A. M. Meier, T. R. Tan, R. Bowler, Y. Lin, D. Hanneke, J. D. Jost, J. P. Home, E. Knill, D. Leibfried, and D. J. Wineland, Phys. Rev. Lett. **108**, 260503 (2012).

[17] C. Langer, R. Ozeri, J. D. Jost, J. Chiaverini, B. DeMarco, A. Ben-Kish, R. B. Blakestad, J. Britton, D. B. Hume, W. M. Itano, D. Leibfried, R. Reichle, T. Rosenband, T. Schaetz, P. O. Schmidt, and D. J. Wineland, Phys. Rev. Lett. **95**, 060502 (2005).

[18] G. Morigi, J. Eschner, and C. H. Keitel, Phys. Rev. Lett. **85**, 4458 (2000).

[19] G. Morigi, Phys. Rev. A **67**, 033402 (2003).

[20] C. F. Roos, D. Leibfried, A. Mundt, F. Schmidt-Kaler, J. Eschner, and R. Blatt, Phys. Rev. Lett. **85**, 5547 (2000).

[21] F. Schmidt-Kaler, J. Eschner, G. Morigi, C. F. Roos, D. Leibfried, A. Mundt, and R. Blatt, Appl. Phys. B **73**, 807 (2001).

[22] S. Webster, Ph.D. thesis, University of Oxford, 2005.

[23] G.-D. Lin, S.-L. Zhu, R. Islam, K. Kim, M.-S. Chang, S. Korenblit, C. Monroe, and L.-M. Duan, Europhys. Lett. **86**, 60004 (2009).

[24] R. Islam, E. E. Edwards, K. Kim, S. Korenblit, C. Noh, H. Carmichael, G.-D. Lin, L.-M. Duan, C.-C. J. Wang, J. K. Freericks, and C. Monroe, Nat. Commun. **2**, 377 (2011).

[25] B. C. Sawyer, J. W. Britton, A. C. Keith, C. C. J. Wang, J. K. Freericks, H. Uys, M. J. Biercuk, and J. J. Bollinger, Phys. Rev. Lett. **108**, 213003 (2012).

[26] R. Islam, C. Senko, W. C. Campbell, S. Korenblit, J. Smith, A. Lee, E. E. Edwards, C.-C. J. Wang, J. K. Freericks, and C. Monroe, arXiv:1210.0142.

[27] C. Monroe, D. M. Meekhof, B. E. King, S. R. Jefferts, W. M. Itano, D. J. Wineland, and P. Gould, Phys. Rev. Lett. **75**, 4011 (1995).

[28] B. E. King, C. S. Wood, C. J. Myatt, Q. A. Turchette, D. Leibfried, W. M. Itano, C. Monroe, and D. J. Wineland, Phys. Rev. Lett. **81**, 1525 (1998).

[29] C. F. Roos, T. Monz, K. Kim, M. Riebe, H. Häffner, D. F. V. James, and R. Blatt, Phys. Rev. A **77**, 040302 (2008).

[30] T. Kampschulte, W. Alt, S. Manz, M. Martinez-Dorantes, R. Reimann, S. Yoon, D. Meschede, M. Bienert, and G. Morigi, arXiv:1212.3814.

[31] K. Xia and J. Evers, Phys. Rev. Lett. **103**, 227203 (2009).